



Stockholm  
University

# Bachelor Thesis

Degree Project in  
Marine Geology 15 hp

## **Eocene-Oligocene Benthic Foraminifera Stable Isotope Stratigraphy and Paleoceanography of ODP Site 757 and 756, Ninetyeast Ridge, Southern Indian Ocean**

Max Holmström



Stockholm 2014

Department of Geological Sciences  
Stockholm University  
SE-106 91 Stockholm

# **Eocene-Oligocene Benthic Foraminifera Stable Isotope Stratigraphy and Paleoceanography of ODP Site 757 and 756, Ninetyeast Ridge, Southern Indian Ocean**

By Max Holmström

## **Abstract**

The EOT is marked by a two-step shift in the  $\delta^{18}\text{O}$  record of benthic foraminifera. The transition was rapid (500 000 years) and occurred roughly 34 million years ago. It marks an important step in Earth's climate history where semi-permanent ice-sheets developed over Antarctica and is considered the initiation of the modern glaciated climate that the Earth experience today. Ninetyeast Ridge is a hot spot trail in the Indian Ocean that was formed by the Keguelen/ Ninetyeast hotspot and was one of the drilling targets of ODP leg 121 and among other sites 757 and 756 were drilled. To gain a better understanding of the paleoceanography and better constrain the timing of the EOT in the Indian Ocean, benthic foraminifera stable isotopes in *Cibicidoides havanensis* was analysed at site 757B and *Cibicidoides mundulus* at site 756C and was then age calibrated using an age model. The results indicate that the significant two-step shift that characterizes the EOT is present at Site 757B. However the results also indicate that it is not sufficient to use an age model that assumes a constant sedimentation rate since it changed drastically at this site at the E-O boundary. Finally the results indicates that there may have been several water masses operating simultaneously in the Indian Ocean at the EOT, the water masses discussed as most likely in this thesis is AAIW and TISW.

# Table of Contents

<b>ABSTRACT</b> .....	<b>1</b>
<b>TABLE OF CONTENTS</b> .....	<b>2</b>
<b>1 INTRODUCTION</b> .....	<b>3</b>
1.1 PREVIOUS RESEARCH AND SPECIFIC AIMS .....	3
<b>2 BACKGROUND</b> .....	<b>5</b>
2.1 THE EOCENE/OLIGOCENE BOUNDARY .....	5
2.2 GEOLOGICAL SETTING AND SITE DESCRIPTION .....	6
2.3 PALEOCEANOGRAPHY AND PALEOCIRCULATION OF THE INDIAN OCEAN .....	7
2.4 STABLE ISOTOPES IN BENTHIC FORAMINIFERA.....	8
<b>3 METHOD</b> .....	<b>10</b>
3.1 SEDIMENT PREPARATION .....	10
3.2 TAXONOMY AND IDENTIFICATION .....	11
3.3 MICROSCOPY, COLLECTION OF SAMPLE MATERIAL .....	12
3.4 STABLE ISOTOPE ANALYSIS.....	12
3.5 SCANNING ELECTRON MICROSCOPE (SEM) .....	13
3.6 DEPTH TO AGE CORRELATION.....	13
<b>4 RESULTS</b> .....	<b>14</b>
4.1 FORAMINIFERA PRESERVATION .....	14
4.2 SEM .....	14
4.3 STABLE ISOTOPES.....	15
<b>5 DISCUSSION</b> .....	<b>19</b>
5.1 IDENTIFICATION OF THE EOT CLIMATIC EVENTS.....	19
5.2 AGE MODEL AND AGE CORRELATION.....	19
5.3 COMPLETENESS OF THE EOT.....	20
5.4 SAMPLING RESOLUTION AND THE Oi-1 SHIFT.....	21
5.5 POSSIBLE ERRORS AND LIMITATIONS.....	22
5.6 GLOBAL AND LONG TERM PERSPECTIVE .....	23
<b>6 CONCLUSIONS</b> .....	<b>24</b>
<b>ACKNOWLEDGEMENTS</b> .....	<b>25</b>
<b>REFERENCES</b> .....	<b>26</b>
<b>APPENDIX</b> .....	<b>28</b>
A. STABLE ISOTOPE DATA .....	28
B MICROSCOPE VIEW OF PICKED BENTHIC SPECIES.....	31

# **Eocene-Oligocene Benthic Foraminifera Stable Isotope Stratigraphy and Paleoceanography of ODP Site 757 and 756, Ninetyeast Ridge, Southern Indian Ocean**

## **1 Introduction**

Roughly 34 million years ago a major shift in the Earth's climate occurred. The Earth transitioned from greenhouse to icehouse climate conditions with permanent glaciers at the South Pole and global cooling. This transition is called the Eocene Oligocene climate transition (EOT) and took roughly 500 000 years to complete (Zachos et al. 1996; Coxall and Pearson, 2007) and marks the end of a 17Ma trend of cooling climate since the early Eocene Climatic Optimum as well as being considered the start of the modern colder climate that is governing on Earth today (Zachos et al. 1996; Zachos et al. 2001).

The EOT is believed to have been caused by a number of factors coinciding, (I) the opening of the oceanic passages that connected Antarctica with Australia and South America, allowing circumpolar currents to form, thus isolating Antarctica from the rest of the climatic system (Kennett, 1977), (II) a slow but steady decrease of atmospheric CO<sub>2</sub> (Zachos et al. 1996; DeConto and Pollard, 2003), (III) the natural variation in the Earth's orbital cycles that changed net insolation and promoted cooler summers, that in return prevented snow and ice from melting thus enabling ice-sheets to grow (Coxall et al. 2005). This knowledge has been acquired by using various paleoclimate proxies were benthic foraminifera has been identified as the most powerful tool for deriving Earth's climate history (Zachos et al. 1992; Coxall and Pearson, 2007).

Antarctic glaciation during the Eocene/Oligocene boundary (E-O boundary) is only directly represented by glaciomarine sediments deposited around Antarctica (Coxall and Pearson, 2007). Therefore to investigate the climate conditions at the E-O boundary it is necessary to make use of geologic records such as benthic foraminifera stable isotopes, that can act as paleoclimate proxies. Proxies are an indirect source of climate information, such as temperature, ice volume and circulation, but they do not control the climate, they merely react to it (Coxall and Pearson, 2007). High resolution stable isotope records and the technical advancements in measuring them has provided valuable insight on how the Earth's climate has developed over a range of time scales from thousands to millions of years (Zachos et al. 2001).

### **1.1 Previous Research and Specific Aims**

A constant goal of research into this time period is to precisely constrain the timing of the EOT while also assessing reproducibility of the EOT benthic foraminifera stable isotope records in several ocean basins and identify their difference. Previous work has answered the more broad questions such as the most likely cause for the EOT (Kennett, 1977; Zachos et al. 1996; DeConto and Pollard, 2003; Coxall et al. 2005) but many more focused questions still remain (Coxall and Pearson, 2007). To answer them it is important to create new high resolution stable isotope records that can resolve more short term variations (Coxall and Pearson, 2007) such as orbital variations that may have played a critical role in the final push that started the EOT (Coxall et al. 2005).

There have been few previous studies of  $\delta^{18}\text{O}$  and  $\delta^{13}\text{C}$  in benthic foraminifera in the tropical Indian Ocean, because of poor preservation and hiatuses in the drilled cores. Therefore most information on E-O boundary come from sediments drilled in the Atlantic, Pacific and southern Indian Ocean. These few studies were still able to confirm that the two step  $\delta^{18}\text{O}$  isotopic shift truly is a global signal found in all major ocean basins, including the tropical Indian Ocean (Zachos et al. 1992).

A considerable weakness of the studies conducted previously in the Indian Ocean by Zachos et al. (1992) is that they are  $\delta^{18}\text{O}$  and  $\delta^{13}\text{C}$  stable isotope records over a considerable amount of time (from early Paleocene to late Miocene) thus making them fairly coarse in resolution. In this thesis it has been attempted to precisely constrain the EOT by using high-resolution sampling over a shorter period of time (a few million years) to improve the understanding of paleocirculation and paleoceanography in the Indian Ocean at this major shift in Earth's climate. In more detail this was done by:

1. Establishing a high-resolution benthic foraminifera isotope record with a sampling resolution of 1 sample every 30 cm for Site 757 to determine how much of the global two step isotopic shift that characterizes the EOT, that is present at this site.
2. Assessing the magnitude of the isotopic shift at this site compared to other ODP sites in the Indian Ocean and globally, and discuss their relation to ocean-climate and carbon system changes at this time.
3. Determine the timing of the EOT climate shift by using detailed age models produced by Tomas Schedwin thesis (2014) using the same samples that was used to produce the stable isotope record used in this thesis.

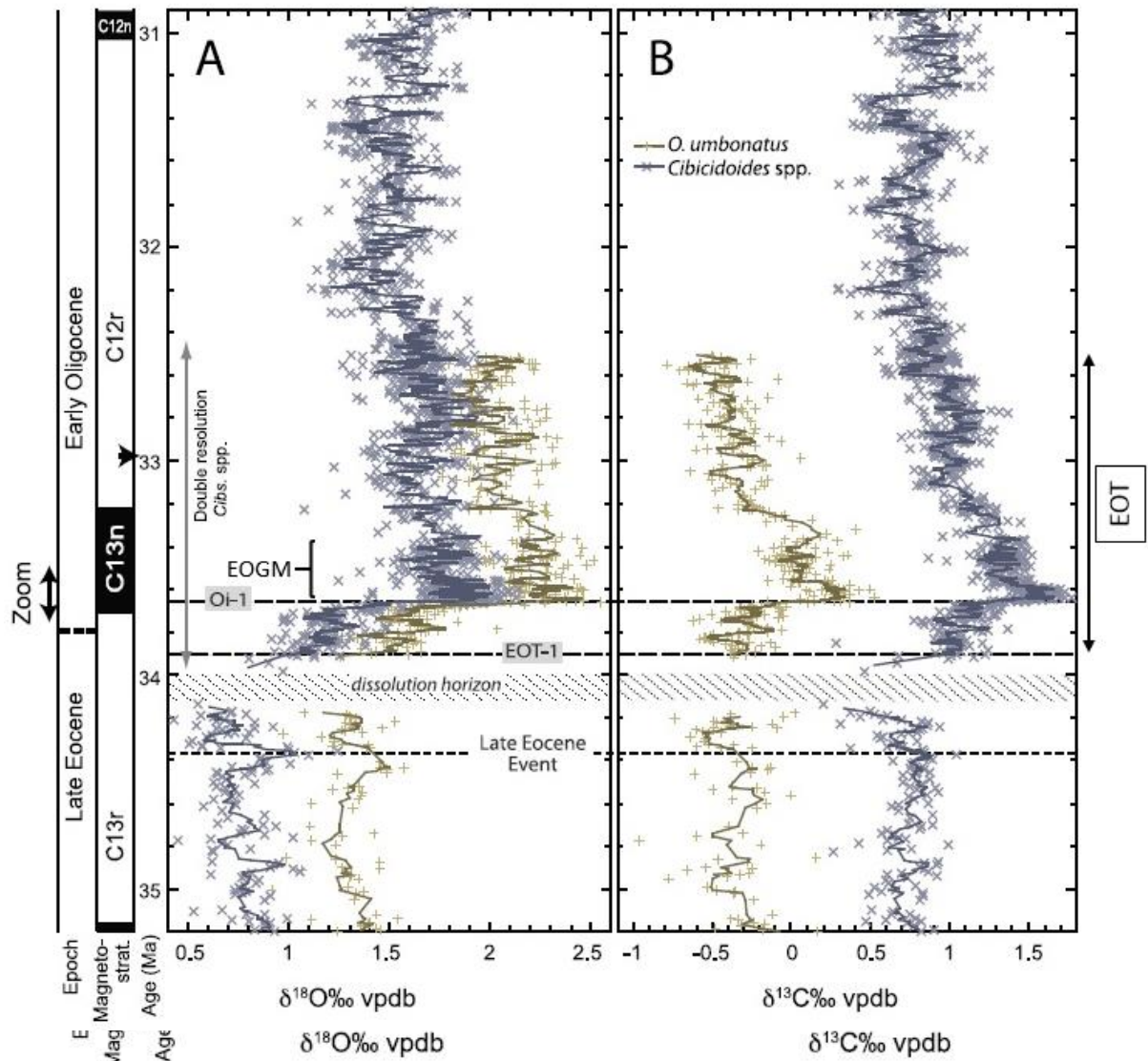


Figure 1. The E-O boundary in benthic foraminifera  $\delta^{18}\text{O}$  and  $\delta^{13}\text{C}$  as recorded at equatorial Pacific ODP Site 1218. This record and the named isotope steps and excursions have been used as template when analysing the records produced in this thesis. Modified from Coxall and Wilson (2011).

## 2 Background

### 2.1 The Eocene/Oligocene Boundary

The E-O boundary is defined by the disappearance of the planktonic foraminiferal family *Hantkenina* that had previously been a minor but important part of assemblages for millions of years prior to the E-O boundary (Coxall and Pearson, 2007). In addition the E-O boundary is marked by a rapid increase ( $>1\text{‰}$ ) of  $\delta^{18}\text{O}$  values in benthic foraminifera (Figure 1) (Coxall and Pearson, 2007) that has been identified as a rapid development of semi-permanent ice-sheets on Antarctica as well as a decrease of deep-water temperatures by at least  $3\text{-}4^\circ\text{C}$  (Zachos et al. 1996).

The EOT however did not occur all at once, instead it was a stepwise transition over several thousands of years. The first step in the transition is defined as the Eocene-Oligocene transition event 1 (EOT-1) (Katz et al. 2008) roughly 34 Ma (Coxall and

Wilson, 2011) (Figure 1) which is marked by a 0.9‰ increase in  $\delta^{18}\text{O}$  values as well as 2.5°C cooling of the deep-water masses. The second step, called the Oligocene Ice Event 1 (Oi-1) (Katz et al. 2008), roughly 33.6 (Coxall and Wilson, 2011) starts after a short period of pre-excursion values that followed EOT-1. This event is characterized by a ~1‰ increase in  $\delta^{18}\text{O}$  values (Katz et al. 2008) and it is this event that marks the initiation of the semi-permanent ice-sheets on Antarctica (Zachos et al. 1996). The final step in the EOT is what is referred to as the Early Oligocene Glacial Maximum (EOGM). This is a zone from roughly 33.6 to 33.2 Ma where the  $\delta^{18}\text{O}$  values are the highest before they eventually start to decline (Coxall and Pearson, 2007).

The ice-sheets on Antarctica had and still have a large impact on the regional and global climate and biology on Earth. The formation of the ice-sheets caused major turnover in both marine and terrestrial ecosystems, forcing biological evolution to develop more cold resistance and adaptations to a more arid climate (Coxall and Pearson 2007). This is a direct result of the glaciers being an enormous heat sink, but at the same time changing land/sea coverage and planetary albedo thus changing continental weathering rates and ocean chemistry in the process (Zachos et al. 1996). Also, the ice-sheets promoted more vigorous circulation; both atmospheric and oceanic causing increased formation of Antarctic Bottom Water (AABW) and at the same time upwelling of nutrient rich waters (Zachos et al. 1996).

## 2.2 Geological Setting and Site Description

As part of the Ocean Drilling Program's (ODP) leg 121, Ninetyeast Ridge was one of the drilling targets. Ninetyeast Ridge is a 5000km long and 100-200km wide bathymetric feature in the Indian Ocean stretching from 32°S to 10°N (Peirce et al. 1989; Royer et al. 1991). It has a relief that varies between 1500m at its lowest and 3000m at its highest. Ninetyeast Ridge is believed to be a hotspot trail of mid-Cretaceous to Oligocene age with increasing age to the north and is believed to be part of a larger igneous province formed by the Kerguelen/Ninetyeast hotspot which also formed Broken Ridge and the Kerguelen-Heard Plateau (Peirce et al. 1989).

Ninetyeast Ridge is made up by basalts that erupted onto the Indian Plate. It is believed that the eruptions took place on young weak oceanic crust due to the isotactic compensation associated with the area. Geochemical data suggests that these basalts erupted in shallow waters or subarially (Peirce et al. 1989) and the shape of Ninetyeast Ridge is a result of the northward movement of the Indian plate over the stationary Kerguelen/Ninetyeast hotspot resulting in a straight north/south pointing ridge (Royer et al. 1991).

Site 757B is located 17°01.458'S, 88° 10.899'E on Ninetyeast Ridge (Figure 2). Drilling at this site recorded a 374.8m long section with a total recovery of 72% meaning that 271.94m of cored material were retrieved (Shipboard Scientific Party, 1989). It was drilled at a depth 1650m and has an estimated paleodepth of 1000m (Figure 3). 200m of that is lower Eocene to Pleistocene ooze (Zachos et al. 1992) with high amounts of foraminifera mixed in with volcanic ash and tuff. The sedimentation rate varies from about 5.5m/m.y. in the Eocene to about 2m/m.y. in the Oligocene (Zachos et al. 1992). Also the site records a history of declining volcanic activity in the area (Shipboard Scientific Party, 1989).

Site 756C is located 27°21.253'S, 87°35.890'E on the southern end of Ninetyeast Ridge (Figure 2) (Shipboard Scientific Party, 1989). This site was drilled at a depth of 1515m and had a paleodepth of roughly 450m (Figure 3). The sedimentation rate for site 756 is estimated to have been stable through Eocene to Pleistocene with rates of >4m/m.y. (Zachos et al. 1992).

### 2.3 Paleoceanography and Paleocirculation of the Indian Ocean

The Indian Ocean worked quite differently at the time prior to the E-O boundary in contrast to today where it is a mixture of several different water masses derived from a number of sources within and outside the basin. Sub-surface water masses today are derived mainly of Antarctic Intermediate water (AAIW) and Antarctic Bottom water (AABW) in combination with minor amounts of other water masses such as North Atlantic Deep-water (NADW) and Red Sea derived saline water. Back at the start of the Eocene the whole of the Indian Ocean is believed to have been quite homogenous in terms of water masses (Zachos et al. 1992).

Deep-water temperatures in the Indian Ocean had been high throughout the Paleocene with temperatures of about 10-11°C. Temperatures peaked in early Eocene rising as high as 14-16°C. At this time it is believed that deep-water did not form in high latitudes as it does today because of low planetary temperature gradients, but instead that it formed in marginal seas with high-salinity. The true location of the deep-water formation in the early Eocene is unknown but the most likely area is the west Tethys Ocean due to its abundance of shallow marine plateaus suitable for high-salinity water formation. However evidence also suggests that deep-water still formed in high latitudes because of similar  $\delta^{18}\text{O}$  values in high-latitude planktonic foraminifera and benthic foraminifera from the Indian Ocean (Zachos et al. 1992).

At 42 Ma a significant shift in the Indian Ocean occurred, the shift caused  $\delta^{18}\text{O}$  values of southern and northern Indian Ocean to diverge. This evidence suggests that a thermal segregation of the intermediate water masses of the Indian Ocean had formed that resulted in two separate water masses, one cool high-latitude water mass, called Antarctic intermediate water (AAIW) and one warm low-latitude water mass, called Tethyan-Indian saline water (TISW). It is believed to have been caused by the widening of the Antarctica and Australia gateway which caused cooling in the higher latitudes of the Indian Ocean, allowing surface waters around Antarctica to become much cooler (<10°C) and as a result was able to sink and form the cool water mass at a greater extent than before. Changes in distribution of planktonic and benthic foraminifera and the disappearance of warm water nannofossils from the southern Indian Ocean further strengthens the evidence for a thermal segregation at this time (Zachos et al. 1992).

Although the event at 42 Ma was important for the structure of the water masses of the Indian Ocean, the most significant cooling event occurred at 34Ma, marked by a ~1‰ increase in benthic foraminifera  $\delta^{18}\text{O}$ , the EOT (Coxall and Pearson 2007). It is confirmed to be the same event identified in the Pacific and the Atlantic by using bio- and Sr stratigraphy and is therefore considered to be a truly global and major event in the climate of this period. The increase in benthic foraminifera  $\delta^{18}\text{O}$  coincides very well with the appearance of ice rafted debris (IRD) at the Kerguelen Plateau (KP) which supports the existence of large ice-sheets. This IRD is carrying a mineral signal that

could only have originated in Antarctica suggesting that these ice-sheets must have been large enough to be able to travel around 1000km from the coast of Antarctica to the KP (Zachos et al. 1992).

Entering the early Oligocene the deep-waters in the Indian Ocean had cooled to about 6-8°C (Zachos et al. 1992). Most of the cooling (~4°C) (Zachos et al. 1992) came from the successive cooling of the deep-waters observed over 10m.y. that ended with rapid cooling of deep-waters and formation of ice-sheets at the E-O boundary. Still the dominant water masses at intermediate depth appear to have been AAIW and TISW but both of these water masses experienced significant cooling across the E-O boundary (Zachos et al. 1992).

## 2.4 Stable Isotopes in Benthic Foraminifera

The term stable isotope is derived from the fact that these elements do not decay into lighter isotopes over time as radioactive isotopes like uranium isotopes or carbon-14 does. When these isotopes take part in the reactions of biological, geological and environmental systems they can be used to track various conditions affecting their surroundings (Nelson Eby, 2004). This is due of the mass difference between the isotope and its lighter counterpart, which in turn affects the speed at which these compounds react. The lighter isotopes react faster, this causes isotopic fractionation and the most important control on the extent of the fractionation is the relative mass difference between the different isotopes. Lighter elements therefore have a larger fractionation than heavier because of the relative mass difference (Nelson Eby, 2004).

Since foraminifera secrete a CaCO<sub>3</sub> shell they will naturally record the isotopic conditions in their environment. When the organism later dies its shell can accumulate on the seafloor and become part of the records that are used today to reconstruct paleoceanographic and paleoclimate conditions (St. John et al. 2012).

### 2.4.1 $\delta^{18}O$

In benthic foraminifera  $\delta^{18}O$  is a very powerful paleoclimate proxy. It is affected by (I) seawater temperature and (II)  $\delta^{18}O$  of seawater. The latter is affected by the growth and retreat of large glaciers (Coxall and Pearson, 2007) because more of the lighter isotopes get locked in the ice due to isotopic fractionation through the hydrological cycle. Through the whole of the Cenozoic  $\delta^{18}O$  changed by of 5.4‰ towards more positive values, ~3.1‰ of this change is thought to be caused by deep-water cooling, ~1.2‰ was from Antarctic glaciation and ~1.1‰ from the northern hemisphere glaciation (Zachos et al. 2001). This means that  $\delta^{18}O$  is a proxy for several climate parameters, firstly it is a proxy for deep-water temperatures and ice volumes, but for the E-O boundary it is also able to constrain high southern latitude surface temperatures, since this was a site of deep-water production (Coxall and Pearson, 2007). This is because most of the deep-water is believed to have been produced in the Southern Ocean close to Antarctica at this time and therefore allowing surface temperatures to be reconstructed from deep-water isotopic data (Wright and Miller, 1993).

### 2.4.2 $\delta^{13}C$

$\delta^{13}C$  is a proxy that record changes in carbon cycling of the surface and deep oceans. It is affected by how much organic carbon is buried and the efficiency of the oceanic carbon pump. At the EOT benthic foraminifera recorded a rapid increase in  $\delta^{13}C$  values

by  $\sim 1\text{‰}$ , peaking at the base of the EOGM and then slowly returning to pre-excursion values. This has been identified as an increase in  $\text{CaCO}_3$  and organic carbon delivery to the seafloor because of the increased primary productivity caused by intensified continental weathering as a result of sea level drop. In combination with increased upwelling caused by intensified wind stress, provided important limiting nutrients to the oceans (Coxall and Pearson, 2007).

In addition  $\delta^{13}\text{C}$  can be used to track direction in which deep-water masses move. This is because a deep-water mass gets more enriched in  $^{12}\text{C}$  as it gets older. This is because of the release of light enriched  $\text{CO}_2$  produced through decomposition of organic material on the seafloor. However, this method assumes that the rain rate of organic carbon is constant, otherwise the signal might get lost in the noise (Zachos et al. 1992).

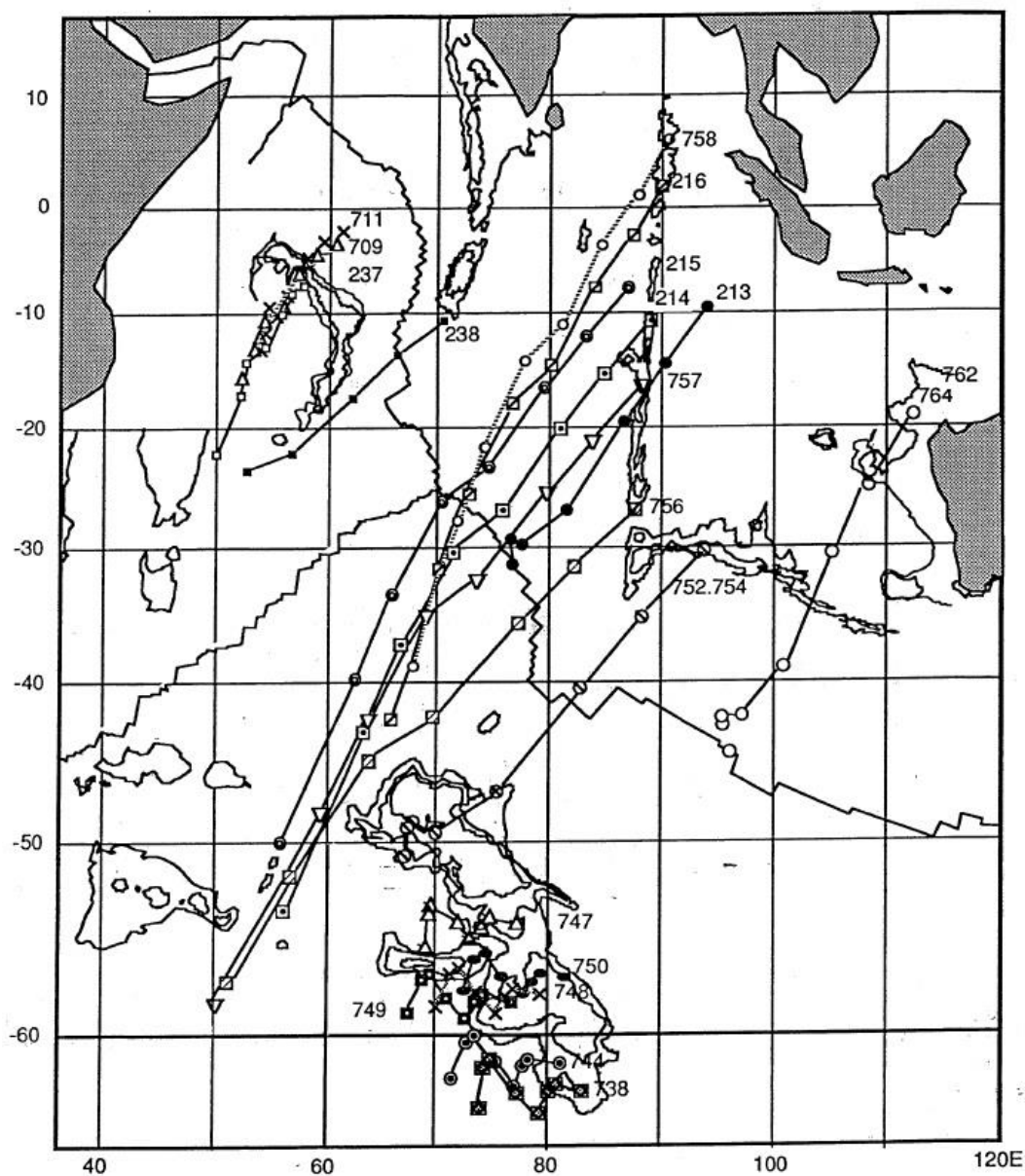


Figure 2. Displays the current position of the Ninetyeast Ridge in relation to continental land masses and other bathymetric features. In addition this Figure also displays the paleopositions of the sites drilled at Ninetyeast Ridge and Broken Ridge, the marker ages are 0, 10, 20, 35, 45, 55, 60 and 66 Ma from current position. From Zachos et al. (1992).

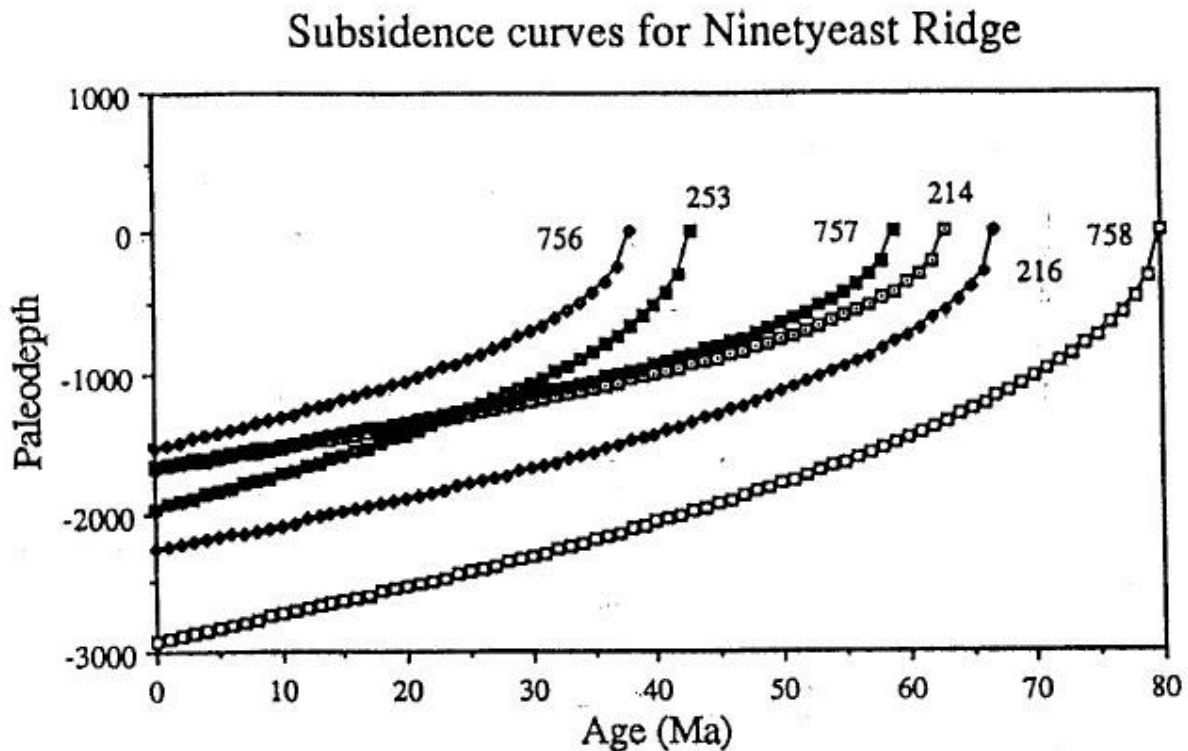


Figure 3. Shows the paleodepth of the various sites drilled at Ninetyeast Ridge, including sites 757 and 756 which are of for this project. From Zachos et al. (1992).

## 3 Method

### 3.1 Sediment Preparation

The foraminifera-containing samples used for this project had already been prepared by S. Bohaty (National Oceanography Centre NOCS, Southampton, UK,) prior to the start of this project the 757B and 756C sediments were washed using a  $>63\mu\text{m}$  sieve and all of the finer material was removed. Therefore it was decided that samples from another site should be washed to get a more complete understanding of the method as a whole.

The sites VAT12 cored in Lake Vättern, central Sweden, and IODP site 1406C were chosen and 10 samples from each site were washed. These samples were first frozen and then freeze dried for 3 days to remove any excess water. Then the samples were moved from plastic bags to Erlenmeyer flasks (E-flask) and the total weight of both the dry sample and E-flask were recorded using a Sartorius LP 220 S balance (1mg resolution), in addition some of the 1406C dry sample was saved for later use because it had a large enough volume to begin with. Each E-flask was filled up to 100ml (for VAT12) and 150ml (for 1406C) with deionized water, and then covered with parafilm.

Samples were then disaggregated in the water on a shaker table at 175rpm for at least one hour, some individual samples were shaken for a longer period of time because it is important to keep the samples moving so that the sample does not settle back down. Then the suspended sample was poured into a  $>63\mu\text{m}$  sieve and both sieve and E-flask was washed with deionized water until all of the clay material was removed and all of the  $>63\mu\text{m}$  material was in the sieve. The samples were then placed in an oven at  $50^\circ\text{C}$

overnight to dry, and in the morning samples were taken out and put in an exicator cabinet to cool down for 1 hour.

New sample vials were weighed with their lid on and then the sample was taken from the sieve to the sample vials using a soft painting brush and a piece of weighing paper. Lastly the vials with the samples are weighed and the dry weight of the  $>63\mu\text{m}$  (sand fraction) was recorded. The sand fraction dry weight is useful for sediment flux studies, however they were not utilized during this thesis project.

### 3.2 Taxonomy and Identification

Benthic foraminifera taxonomy was based on “Cenozoic Cosmopolitan Deep-Water Benthic Foraminifera” by van Morkhoven et al. (1986) and “Oligocene to Pleistocene Benthic Foraminifer Assemblages at Sites 754 and 756, Eastern Indian Ocean” by Nomura et al. (1991). Two benthic foraminifera species were identified as most appropriate for stable isotope analysis, *Cibicidoides havanensis* and *Cibicidoides mundulus*, in addition *Gyroidinoides sp.* was identified for later chemical analysis, (requested by S. Bohaty, NOCS). An important reason to why these particular species were chosen is that they are epifaunal (living on the seafloor) and abyssal (Morkhoven et al. 1986). Epifaunal species are believed to record deep-sea conditions better than infaunal and the abyssal species are largely unaffected by the changed living conditions across the E-O boundary (Coxall and Pearson 2007) allowing mono-species analysis through the whole section studied. Also this taxon has been widely used in previous EOT studies allowing direct comparison between stable isotope records from different sites.

*Cibicidoides havanensis* (Cushman and Bermúdez 1937) (Appendix B) was identified using its convex spiral side seen from edge view, where the spiral side is more convex than the umbilical side, you can see it since it is very unstable if it is positioned on its spiral side, in addition there are many large pores on the spiral side that are visible in the microscope and these pores are oriented in a spiral. On the umbilical side the sutures are clearly visible and it has 12 chambers in the final whorl on this side there are also pores visible but they are oriented in lines going from the edge of the test towards the middle. The aperture is quite thin and bend upwards from the umbilical side to the spiral side. *Cibicidoides havanensis* has a very round test and is trochospiral.

*Cibicidoides mundulus* (Brady, Parker and Jones 1888) (Appendix B) can be recognized by its biconvex test that is evenly convex on both the spiral and umbilical side. The test is sub-rounded and is elongated in one axis (y or x depending on how it is oriented). It has a distinct keel seen in edge view and is trochospiral. The umbilical side has clearly visible sutures that are bent slightly inwards and in the final whorl supports 10-12 chambers. The spiral side has pores that are visible in microscope, but the most distinctive feature of the spiral side is that there are sutures visible on this side as well as on the umbilical side, but this time they are oriented around a quite circular core of the test that is slightly elevated.

*Gyroidinoides sp.* (Appendix B) has a very smooth test when looking in the microscope, this made it quite easy to spot amongst other foraminifera in the samples. The umbilical side is convex and the test is very smooth. The spiral side is flat with a distinct spiral visible in microscope, the test is smooth even in this view. Additionally it has a very

distinct angular edge view having a slight triangular shape with a rounded base. No sutures can be seen while looking in the microscope or electron microscope.

### 3.3 Microscopy, Collection of Sample Material

Benthic foraminifera samples were picked by hand using a small paint brush dipped in water. The size fraction picked was 250-500 $\mu\text{m}$ , this was to get as close as possible to the 212-355 $\mu\text{m}$  size fraction, which S. Bohaty (Southampton) used when he picked 25 out of the 63 of the 757B samples, with the sieves available at the Department of Geological Sciences (IGV) at the time. In addition some of the first samples were picked in the >150 $\mu\text{m}$  and 150-250 $\mu\text{m}$  size fractions, but these smaller fractions was abandoned because they were not yielding enough material and was therefore not time efficient. The benthic foraminifera species picked for stable isotope analysis at site 757B and 756C was *Cibicidoides havanensis* and *Cibicidoides mundulus*.

### 3.4 Stable Isotope Analysis

Picked mono-species benthic foraminifera samples were weighed using a Sartorius MC5 microbalance (0.001 mg resolution). The aim was to have all the samples weighing around 0.2mg, but not lower than 0.1mg and not above 0.3mg, because of the lowest and highest detection limit of the mass spectrometer. 3 benthic foraminifera specimens were used whenever possible, but in some cases this was not possible since the foraminifera was too heavy and in these cases only 2 specimens had to be used. In addition the samples were analysed in random order to prevent any analytical drift in the mass spectrometer that can occur if all samples are analysed in succession.

For site 757B *Cibicidoides havanensis* was chosen as the main species for analysis because it was abundant in the samples and it was one of the species that Steven Bohaty had picked when he worked with the 757B samples earlier. However 5 samples of *Cibicidoides mundulus* was also analysed to see if there was any notable difference in the stable isotope values between these two species. In addition to compensate for internal variation (since the amount of specimens used only was 2 or 3) 5 extra samples of *Cibicidoides havanensis* was analysed to see if there was any noticeable internal variation between individual specimens.

At site 756C *Cibicidoides mundulus* was chosen as the main species for analysis, this was because there was almost no *Cibicidoides havanensis* available in these samples and those that were would not have been enough to perform the stable isotope analysis. This however was not considered to be a problem since *Cibicidoides mundulus* have been used successfully in previous studies and would make comparison with other sites easier. In addition the 756C samples were not expected to cross the Eocene/Oligocene boundary and was instead analysed to see if there was any difference between the baseline signals at both sites.

Before analysis samples were first dried in an oven at 50° over the weekend to remove any excess water. Then 100 $\mu\text{l}$  of 99% phosphoric acid was added to the side of the sample vial, not in contact with the sample, and the vial was then flushed with helium gas for 10 minutes. Then the vial was then stood upright to let the acid and samples react overnight.

The stable isotope analysis was performed at the IGV stable isotope laboratory. The setup in the laboratory was comprised of a MAT252 mass spectrometer from Termoscientific and a GasBench II flow preparation and inlet system. The samples were measured against the international standard VPDB. The reproducibility of the method used is 0.07‰ for  $\delta^{13}\text{C}$  and 0.15‰ for  $\delta^{18}\text{O}$ .

### 3.5 Scanning Electron Microscope (SEM)

To gain a better understanding of the diagnostic morphologic features of the most important species for this study (*Cibicidoides havanensis*, *Cibicidoides mundulus* and *Gyroidinoides* sp) and to be able to briefly assess the preservation of the samples images were taken using a Philips XL-30-ESEM-FEG scanning electron microscope (SEM). First the foraminifera specimens were mounted on top of a SEM-stub in three diagnostic positions as shown in Morkhoven et.al. (1986), the specimens were then gold coated to lead away the electrons from the sample preventing them from being electrically charged. Then the samples were imaged under high vacuum ( $>10^5$  millibar) using the SEM.

### 3.6 Depth to Age Correlation

Depth was converted into age using an age model (Figure 4) produced by Tomas Schedwin thesis, (2014) where he converted depth to age by investigating the disappearance and appearance of key planktonic foraminifera species, combined with nanofossil bio-events and previously calibrated ages to produce an equation (equation 1) that could be used to calculate ages for any specific depth at 757B. This equation was then used to correlate depth with ages for the isotope data produced in this thesis. Schedwin also investigated the last occurrence of *Hantkenina* Sp. to be able to determine the E-O boundary at site 757B.

$$\text{Age (Ma)} = 0.3452 * \text{Depth(mbsf)} - 8.157 \quad (1)$$

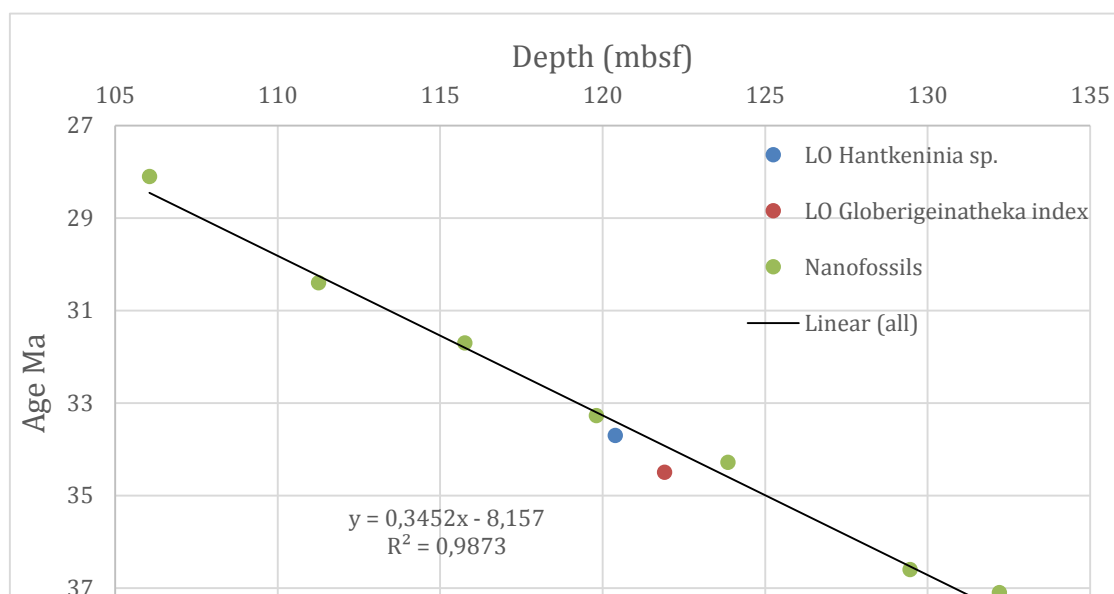


Figure 4. The age model for Site 757B that was used to correlate the depths with ages. This age model was produced by T. Schedwin (2014) using the same samples that were used for stable isotope analysis in this thesis.

Equation 1 was produced using a linear fit through the data points for correlation. This assumes a constant sedimentation rate for the studied interval and should be taken into consideration when the data is analysed.

For Site 756 there was no age model was available so direct depth to age correlation was not possible for the records produced in this study. However to get an approximate age constrain on the 756 data isotopic events were correlated to the 757B age correlated records since the events were assumed to have occurred simultaneously.

## 4 Results

A total of 63 samples were analysed for site 757B, 10 of those samples were analysed twice (Appendix A) to investigate sample reproducibility and cross species comparison. The samples range from 110.55mbsf to 129.54mbsf and the sampling resolution is about 1 sample per 30cm. For site 756C a total of 20 samples were analysed. The samples range from 124.8mbsf to 142.65mbsf with a sampling resolution of about 1 sample per 80-100cm.

### 4.1 Foraminifera Preservation

Site 757B generally show whole and well preserved benthic foraminifera specimen, however a few of them were fractured and broken into mostly large fragments. Generally *Cibicidoides spp.* is numerous but declining down in the section, while *Gyroidinoides sp.* varies between moderate to rare in the entire section. The amount >63µm of sediment in the sample vials is by my assessment quite small but definitely containing enough benthic foraminifera for analysis.

Site 756C sediment samples were also generally well preserved with mostly whole benthic foraminifera specimen, although not as well preserved as 757B. At this site there was more evidence of recrystallization, for example some of the benthic foraminifera had large lumps of CaCO<sub>3</sub> on them that are not part of their shell. In addition there was moderate amounts of pyrite formation on the planktonic foraminifera at this site. The abundance of *Cibicidoides sp.* was much lower than at 757B and *Gyroidinoides sp.* was rare to extremely rare, resulting in that for some samples only 2-3 specimens could be retrieved. However the total amount of >63µm sediment in the vials was much larger than 757B. This was because there were more planktonic foraminifera compared to 757B.

### 4.2 SEM

#### 4.2.1 Site 757B

SEM images (Figure 5) confirms the light microscope visual interpretation that the benthic foraminifera *Cibicidoides havanensis* and *Cibicidoides mundulus* as well as *Gyroidinoides sp.* are generally well preserved in the 757B samples. The only evidence for dissolution found is that some of the pores appear to be filled by calcareous material to some extent and the granular surface, which indicates micron-scale recrystallization typical for deep-sea benthic foraminifera recovered from calcareous ooze.

The tests of the samples are very similar for all 3 species that were imaged looking quite like it is made up by grains of CaCO<sub>3</sub> close up view. Even though the tests of the *Cibicidoides* species studied look quite different from the *Gyroidinoides* when looking in a light microscope.

#### 4.2.2 Site 756C

SEM images (Figure 6) of one species of benthic foraminifera, *Cibicoides mundulus* investigated at site 756C. There seem to be little difference in preservation between site 757B and 756C from what you can see in the SEM pictures. However the most striking difference is that the pores of the foraminifera are more in-filled at this site than could be observed at site 757B. This is consistent with the visual interpretations from this site, suggesting more dissolution at this site. However the surface of the test is less granular suggesting a smaller amount of micron-scale recrystallization at site 756C compared to 757B.

### 4.3 Stable isotopes

#### 4.3.1 Site 757B $\delta^{18}\text{O}$

The new stable isotope analysis show that  $\delta^{18}\text{O}$  (Figure 7) increases in *Cibicoides havanensis* from the deepest to the shallowest sample measured, from  $\sim 1.2\text{‰}$  to  $\sim 2\text{‰}$ , an increase of  $\sim 0.8\text{‰}$ .  $\delta^{18}\text{O}$  variability around the baseline over the measured interval is  $\sim 0.2\text{‰}$ . At 123mbsf an excursion of  $\sim 0.2\text{‰}$  starts towards heavier  $\delta^{18}\text{O}$  that ends at 120mbsf. At 119mbsf another excursion towards heavier values starts and at 117mbsf it ends. This excursion changes the isotopic values with  $\sim 0.6\text{‰}$ . The large excursion is then followed by a period of increased variability of  $\sim 0.4\text{‰}$  from 117mbsf to 115mbsf where it returns to a new baseline variability of  $\sim 0.2\text{‰}$ . There are two relatively stable zones that can be identified, first from 130mbsf to 123mbsf that has  $\delta^{18}\text{O}$  values of  $\sim 1.2\text{‰}$  to  $\sim 1.4\text{‰}$ , the second begins after the zone of maximum values, it stretches from 117 mbsf to the top of the studied interval. The values in this zone are stable at  $\sim 1.8\text{‰}$  to  $\sim 2.0\text{‰}$ , indicating that both stable zones have  $\sim 0.2\text{‰}$  in baseline variability.

The 5 *Cibicoides mundulus* samples (Figure 7) have similar isotopic values to *Cibicoides havanensis*. The 3 top samples are within the range of variability while the 2 samples deeper in the core are  $\sim 0.2\text{‰}$  higher from corresponding *Cibicoides havanensis*. The *Cibicoides havanensis* comparison show little difference from the original samples. Only one data point is outside the expected range, at  $\sim 127$  mbsf with a  $\delta^{18}\text{O}$  value of  $\sim 1\text{‰}$ , suggesting that this data-point may be a false value.

#### 4.3.2 Site 757B $\delta^{13}\text{C}$

$\delta^{13}\text{C}$  in *Cibicoides havanensis* decreases overall from the deepest to the shallowest sample (Figure 7), the values decrease with  $\sim 0.2\text{‰}$  over the sampled section. At 123mbsf a brief excursion towards lighter  $\delta^{13}\text{C}$  values start. The values change from  $\sim 1.2\text{‰}$  to  $\sim 0.7\text{‰}$  a decrease of  $\sim 0.5\text{‰}$ . The excursion is over at 122mbsf. The main feature of the record is an excursion at 120mbsf of  $\sim 0.7\text{‰}$ , towards heavier values, the values change from  $\sim 1\text{‰}$  to  $1.7\text{‰}$ . This excursion ends at about 117mbsf and is followed by a period in the record of declining  $\delta^{13}\text{C}$  values with some brief increases in variability at 115mbsf and 112mbsf to the uppermost sample.

Comparison with *Cibicoides mundulus* yielded no large noticeable differences in  $\delta^{13}\text{C}$  values. They plot within expected variability and does not seem to have any different pattern than *Cibicoides havanensis*. The *Cibicoides havanensis* comparison shows little difference in internal variation, the samples plot within the same range as the original samples.

#### 4.3.3 Site 756C $\delta^{18}\text{O}$

The  $\delta^{18}\text{O}$  of *C.mundulus* values of site 756C (Figure 8) starts out at values  $\sim 1\text{‰}$  and end at roughly  $1\text{‰}$  again at the top. There are two notable excursions in  $\delta^{18}\text{O}$  one at 136mbsf that changes the isotopic composition towards lighter values by  $\sim 0.5\text{‰}$ . The other excursion starts at 130mbsf and changes  $\delta^{18}\text{O}$  towards lighter values again, this time by about  $\sim 0.3\text{--}0.4\text{‰}$ . Compared to the 757B record (Figure 7) the absolute values of  $\delta^{18}\text{O}$  at Site 756C is lower. At Site 756C the maximum values are  $\sim 1\text{‰}$  which is the absolute lowest values at site 757B. The magnitude of the variability appears to be larger than at 757B, with a magnitude of  $\sim 0.4\text{‰}$ .

#### 4.3.4 Site 756C $\delta^{13}\text{C}$

The  $\delta^{13}\text{C}$  values measured in *C.mundulus* (Figure 8) starts with an increase in  $\delta^{13}\text{C}$  values of about  $0.4\text{‰}$ . Values are then somewhat stable from 135 to 130mbsf were another excursion starts, this time towards lighter values. The excursion lowers values by  $\sim 0.3\text{‰}$  but then the values seem to be returning towards heavier values rapidly. Compared to Site 757B the absolute values  $\delta^{13}\text{C}$  are about the same, varying around  $1.2\text{‰}$ . However the magnitude of the variability appears to be higher in  $\delta^{13}\text{C}$  at Site 756C as well as  $\delta^{18}\text{O}$ .

In addition Helen Coxall (Stockholm University SU, Stockholm, Sweden) (personal communication) informs that *Hantkenina* occur throughout the measured interval indicating that the samples are late Eocene in age, and therefore does not capture the EOT. Since the last occurrence of *Hantkenina* marks the E-O boundary (Coxall and Pearson 2007).

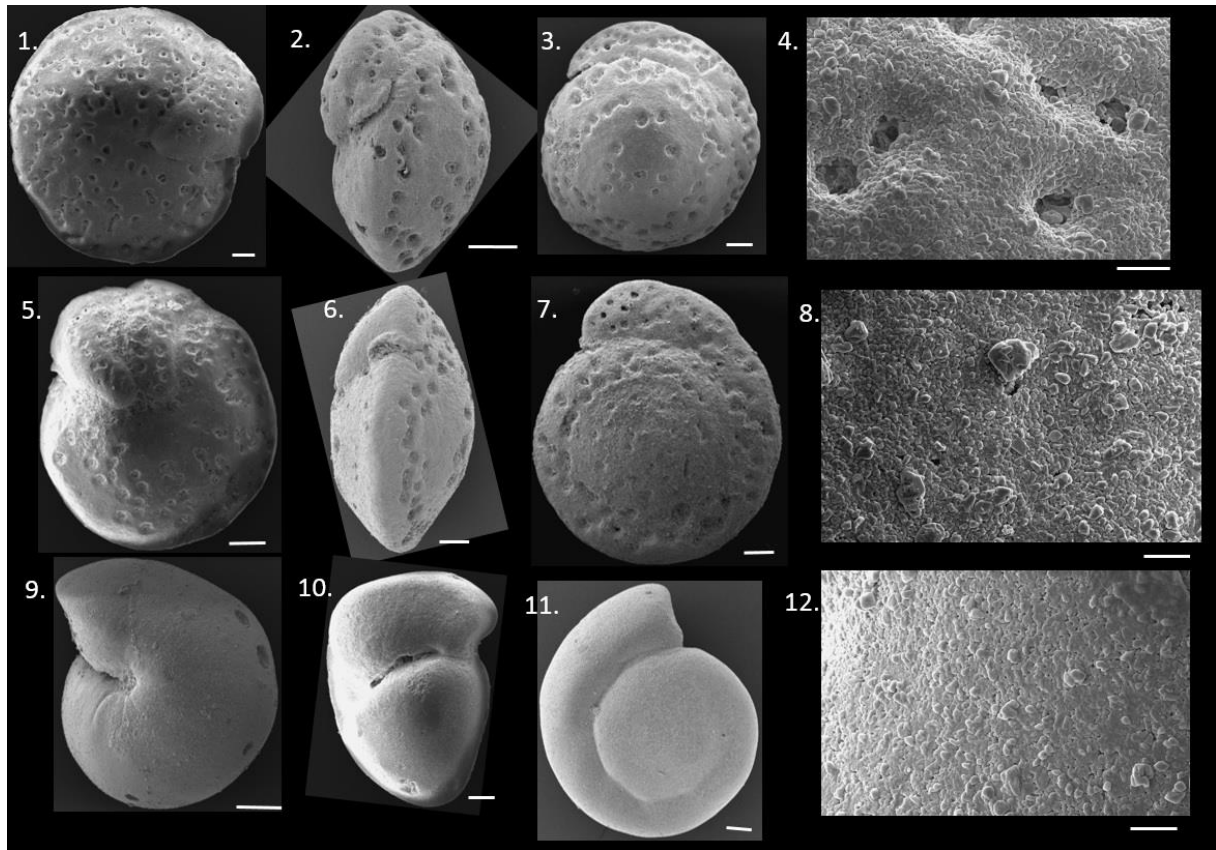


Figure 5. SEM-images of benthic foraminifera at Site 757B, oriented showing umbilical side, edge view and spiral side followed by a picture of the wall textures. The displayed species are 1 to 4 *Cibicidoides havanensis*, 5 to 8 *Cibicidoides mundulus* and 9 to 12 *Gyroidinoides Sp.* Scale bar equal to 100 $\mu$ m except for wall-texture images (4, 8, 12) where it is 20 $\mu$ m. The diagnostic views are represented by different specimens.

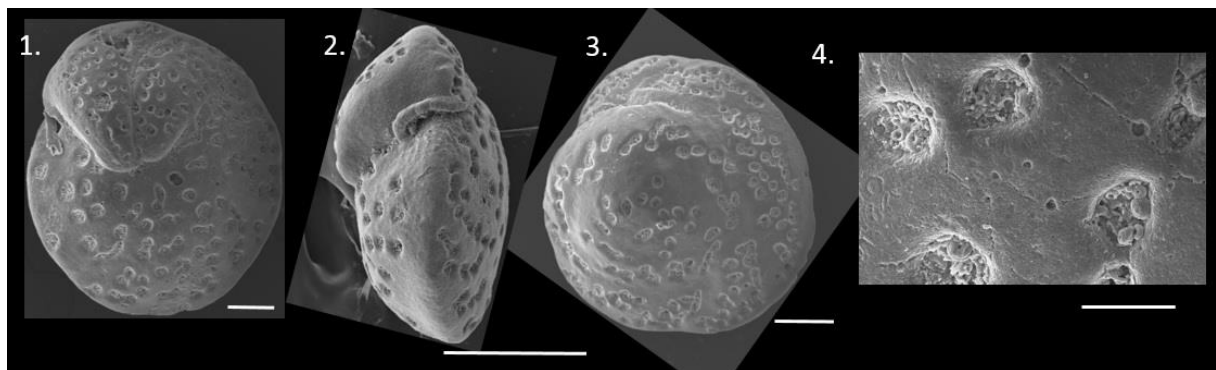


Figure 6. SEM-images of *Cibicidoides mundulus* at Site 756C, oriented showing (1) umbilical side, (2) edge view and (3) spiral side followed by (4) wall textures. Scale bar equal to 100 $\mu$ m except number for which is 40 $\mu$ m, The diagnostic views are represented by different specimens.

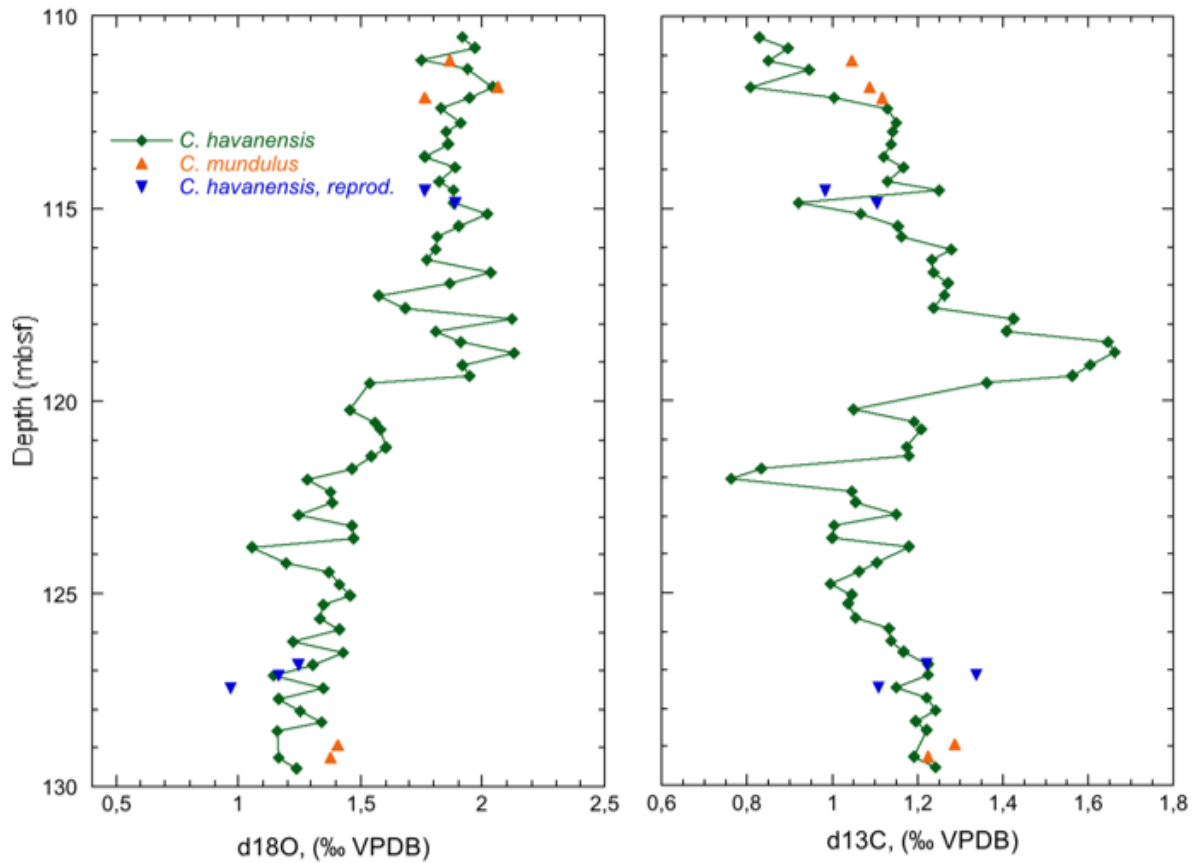


Figure 7.  $\delta^{18}\text{O}$  and  $\delta^{13}\text{C}$  stable isotope records in benthic foraminifera vs depth at site 757B measured in *Cibicides havanensis*. Including the comparison with *Cibicides mundulus* and the extra *C. havanensis* samples for variation comparison

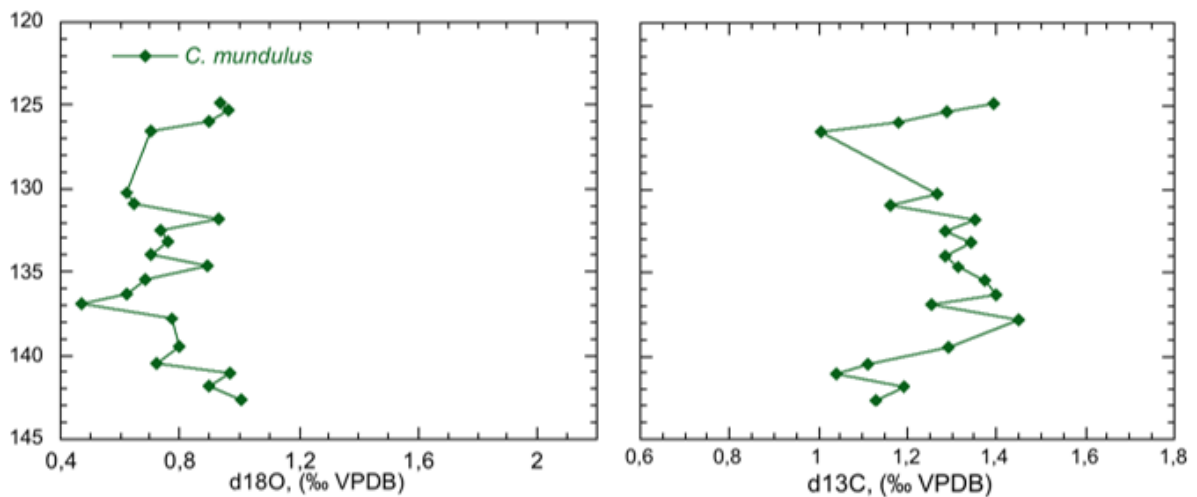


Figure 8.  $\delta^{18}\text{O}$  and  $\delta^{13}\text{C}$  stable isotope records in benthic foraminifera vs depth at site 756C measured in *Cibicides mundulus*.

## 5 Discussion

### 5.1 Identification of the EOT Climatic Events

The climatic events of the EOT were established for Site 757B (Figure 9) using the benthic foraminifera isotope record produced by Coxall and Wilson (2011) at Site 1218, equatorial Pacific and the definition of the EOGM from Coxall and Pearson (2007) (Figure 1) in combination with the descriptions of the events from Katz et al. (2008). Through this comparison the same events identified by Coxall and Wilson (2011) can be recognized at Site 757B.

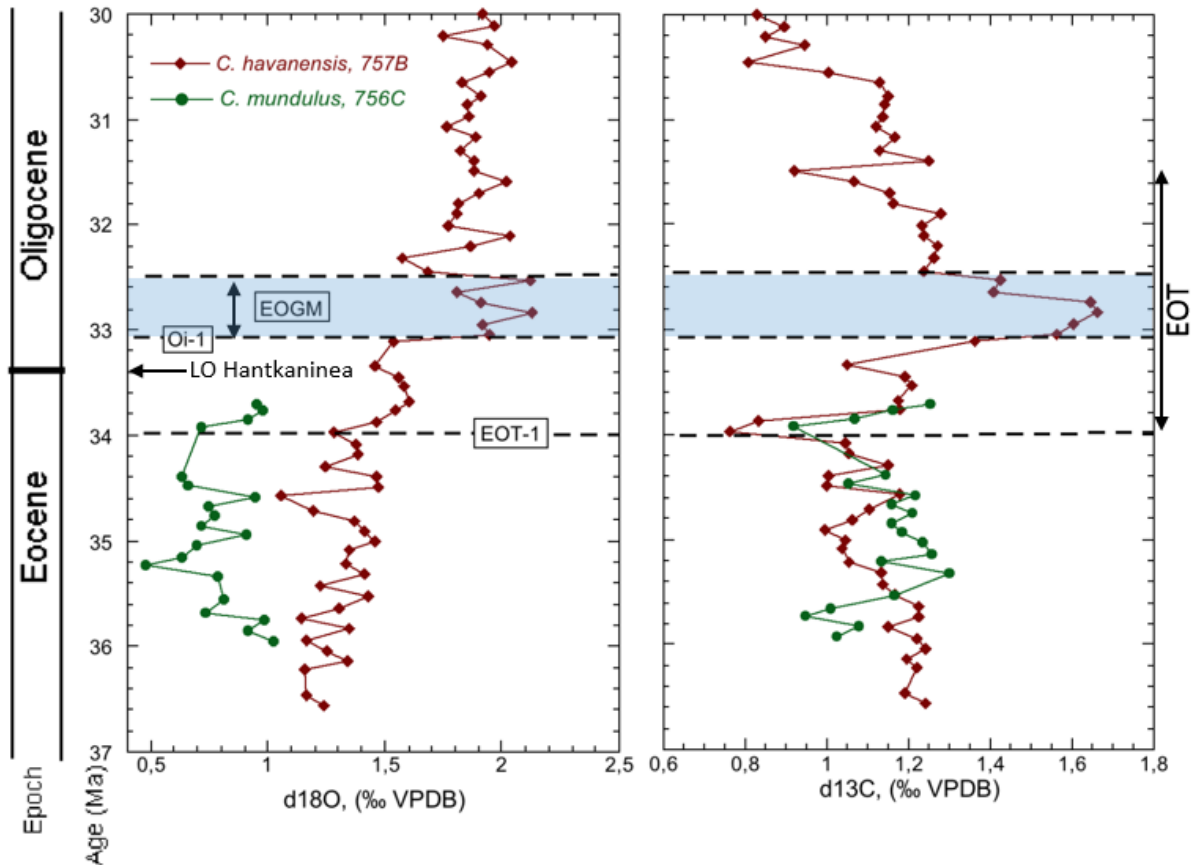


Figure 9. Age calibrated benthic foraminifera stable isotope records from site 757B measured on *C. havanensis*. Also added on are the important climatic horizons, interpreted in this study that has been established for the EOT. When producing this Figure Coxall and Wilson (2011) was used as reference for the positions of Oi-1 and EOT-1 and Coxall and Pearson (2007) for the EOGM. The E-O boundary is marked by *Hantkenina* last occurrence (LO) established at Site 757B by T. Schedwin thesis (2014). In addition an approximate age calibration of isotope data on *C. mundulus* at Site 756C is displayed, based on visual correlation of isotopic events. Note that absolute isotope values for Site 756C may not be exact in this figure.

### 5.2 Age Model and Age Correlation

When an age model is applied to the benthic foraminifera stable isotope data the results turn out like Figure 9. This gives an opportunity to explore the timing compared to the stable isotope records produced by Coxall and Wilson (2011) (Figure 1) the isotope data in this study differ in age. The age model appears to have worked well through the late Eocene were the ages of important events are similar to Coxall and Wilson (2011). However after the EOT-1 boundary the ages appear to be stretched out at Site 757B compared to Site 1218 reference curve, for example the whole of the EOT lasts for 1.5m.y. in the new data, but only for 500k.y. in Coxall and Wilson's (2011) record.

This stretching of the ages may be due to a weakness in the age model. The age model assumes a constant sedimentation rate. According to Zachos et al. (1992) the sedimentation rate at 757B changed at the E-O boundary, from 5.5m m.y.<sup>-1</sup> in the Eocene to 2m m.y.<sup>-1</sup> in the Oligocene. Having a slower sedimentation rate than the new linear age model would cause the ages to stretch and therefore create an offset compared to the reference. Since the much shorter duration of the EOT is supported by several more records (Zachos et al. 1992; Coxall, 2005; Coxall and Pearson 2007; Coxall and Wilson 2011) it is most likely that the difference in duration seen in these new records are due to the problem discussed above.

### 5.3 Completeness of the EOT

The distinctive two step isotopic shift that characterize the EOT is definitely visible at Site 757B (Figure 9) when the record is compared to Coxall and Wilson (2011). In the records it appears as if  $\delta^{18}\text{O}$  values stabilized at a new equilibrium after the EOT which was about 0.5‰ heavier than before. This suggests that the ice-sheets were stable in the Oligocene or that the temperatures of the deep-waters permanently changed. Previous research reveals that the signal is a combination of both cooling and ice formation (Zachos et al. 1996) and IRD with the mineralogical signal from Antarctica is very strong evidence that permanent ice-sheets were present at the time (Coxall and Pearson, 2007). Ice-isotope mass balance estimates suggest that neither ice nor bottom water cooling is strong enough to account for the massive shift alone (Coxall et al. 2005).

The total magnitude of the EOT isotopic shift at site 757B is a 0.8‰ increase in  $\delta^{18}\text{O}$  values. This is slightly lower than the suggested average of ~1‰ increase (Coxall and Pearson, 2007). This value is also lower than the 1.2‰ that Zachos et al. (1992) recorded at site 757.

The  $\delta^{13}\text{C}$  data (Figure 9) displays the two step isotopic shift of the EOT. But the values does not stabilize at a new equilibrium after the shift like the  $\delta^{18}\text{O}$  values do. Instead they return to the old baseline values that governed prior to the EOT boundary. This might suggest that the global carbon cycle were affected by the significant turnover that occurred at the EOT, with increased marine carbon transport (Coxall and Pearson, 2007), but was not fundamentally altered like the  $\delta^{18}\text{O}$  proxy was by the permanent ice-sheets, and recovered to a pre-event state ~500 000 years after the maximum  $\delta^{13}\text{C}$  value was reached.

There is however difference between the  $\delta^{18}\text{O}$  values of the short record analysed at site 756C and Site 757B (Figure 7 and 8). Generally the values at site 756C are isotopically lighter by 0.5‰ compared to 757B. This suggests that temperatures could have been higher at 756C than at 757B. There might be a difference in temperature because of the difference in paleodepth at the two sites, site 757B has a paleodepth of 1000m and 756C a paleodepth of 400m. Suggesting that maybe there are different water masses operating at those depths or that there is a temperature gradient between 400 and 1000m.

The argument for two different water masses is however not supported by the  $\delta^{13}\text{C}$  data since it is very similar values between site 757B and 756C. This leaves the temperature gradient between the depths as one possible explanation to the difference however

there is no mention of any difference in the previous research that would support this theory either.

#### 5.4 Sampling Resolution and the Oi-1 Shift

Zachos et al. (1992) claims that the  $\delta^{18}\text{O}$  in benthic foraminifera shift at Oi-1 is larger if the sampling resolution is high. Zachos determined that the isotopic shift at high resolution is 1.6 to 1.8‰ were as in low resolution it is not above 1.2‰. The explanation by Zachos suggests that one needs a high enough sampling resolution to capture the full magnitude of the Oi-1 isotopic shift. The sites that was analysed in that particular study was 744 and 748 (high resolution, roughly 1 every meter) as well as 757 and 756 (low resolution, 1 sample every 3m). The data produced in this thesis does not however support this claim. At site 757B a total increase of  $\sim 0.8\text{‰}$  is measured even though the sampling resolution is high. This suggests that there might be some other reason to why the isotopic shift is larger at the sites Zachos studied with higher resolution.

Instead the reason for the difference in magnitude of the Oi-1 may be explained by the properties of the two intermediate water masses, AAIW and TISW that has been suggested to operate within the Indian Ocean at the E-O boundary (Zachos et al. 1992). Zachos suggests that AAIW may have stretched as far north as  $45^{\circ}\text{S}$  at this time. It appears that both site 744 and 748 were below  $45^{\circ}\text{S}$  and that Site 757 and 756 were above (Figure 10). This in combination with their paleodepth, which places them in the intermediate water-mass range, suggests that there were differences in the properties between AAIW and TISW.

AAIW forming close to the rapidly cooling Antarctica may have been affected more by the cooling continent than TISW which is believed to have formed much closer to the equatorial region. This in turn caused the difference in  $\delta^{18}\text{O}$  values recorded by benthic foraminifera at Ninetyeast Ridge and the more southern sites since larger shift suggests more cooling of the water mass assuming the ice signal is constant at both locations.

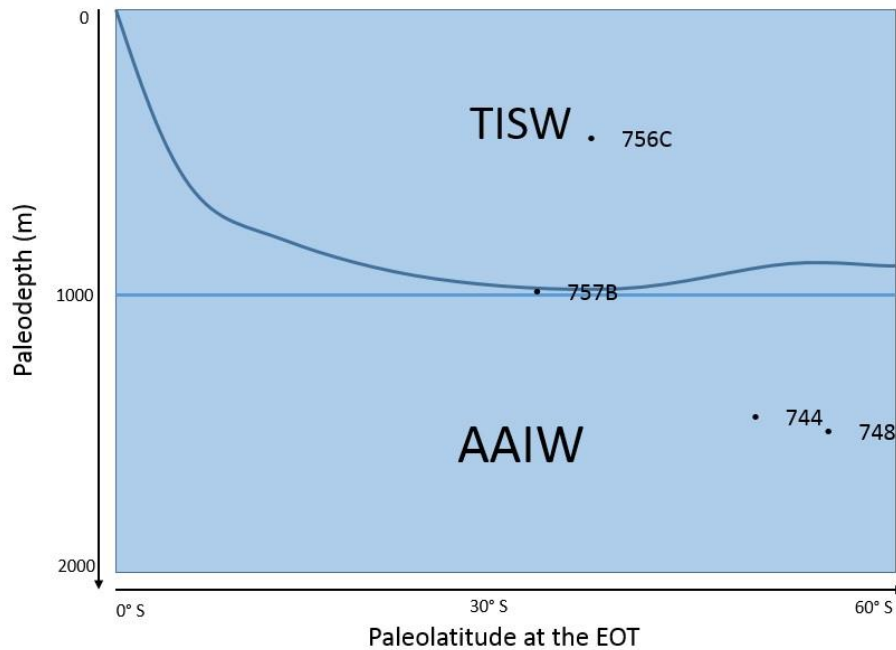


Figure 10. A schematic illustration of how the Indian Ocean may have looked like at intermediate water depth during the EOT with the sites studied in this thesis as well as some of the site studied by Zachos et al. (1992). Paleodepth and latitude information from Zachos et al. (1992).

### 5.5 Possible Errors and Limitations

When working with micropaleontology a considerable weakness in the method is always that the taxonomy and identification of benthic foraminifera species is an interpretation. This means that experience plays a significant role in making sure that the right species are found and picked out. Therefore it might be very hard for someone working with the subject for the first time to pick the right species every time. The reality of the situation is therefore that some mistakes may have occurred during the sampling procedure which may later have affected the final results.

Another important factor that may affect the results is the analytical variation between benthic foraminifera samples made up of multiple specimens. Ideally one would want to use as many specimens as possible to compensate for intersample variation, resulting from sediment mixing. However the weight of the foraminifera specimen and the limitations of the method of the mass spectrometer made it impossible to use more than 3 even going down to 2 specimens in some cases. However the extra *Cibicidoides havanensis* samples (Figure 7) indicate that the individual variation at this site is low since they have very similar values to the original samples.

The comparison with 5 *Cibicidoides mundulus* samples suggests that it would be possible to compare values measured on *C. havanensis* to those of *C. mundulus*. The values of *C. mundulus* are within the range of inter-sample variability through the record. If this true for all *C. mundulus* is not possible to say from this small comparison alone but it indicates that it may be possible to compare the stable isotope values of these two species between other sites were one might be available but not the other.

## 5.6 Global and Long Term Perspective

When the stable isotope data is put into a larger perspective (Figure 10) as in Zachos et al. (2001) it is possible to discuss the long term global effect that the EOT had on Earth's climate. The long term  $\delta^{18}\text{O}$  curve appears to suggest that on a geologic time scale the whole of the Oligocene was an excursion that returned to pre-excursion values that was followed by additional cooling of the climate. This might indicate that the climate conditions that formed at the EOT was not stable on a longer time scale, since at the start of the Miocene the values in Zachos et al. (2001) stable isotope curve has a similar but opposite  $\delta^{18}\text{O}$  shift.

The  $\delta^{13}\text{C}$  curve (Figure 10) however appears to be more stable on the longer time scale. This may well indicate that the global carbon cycle is resilient to climatic changes, since productivity is affected at the event but usually returns to the same values as before after some time. This is supported by the new data produced at 757B, which is very short term but still indicates a stabilization of the carbon cycle after the EOT which was a global event. The reorganization of many of Earth's ecosystems at the EOT (Coxall and Pearson, 2007) may explain why the  $\delta^{13}\text{C}$  values are offset for a time, but as the ecosystems adapt to their new living conditions they can return to the same efficiency as they had before. If the same mechanism can be applied to other events as well it may explain the long term more stable trend of the  $\delta^{13}\text{C}$  curve by Zachos et al. (2001).

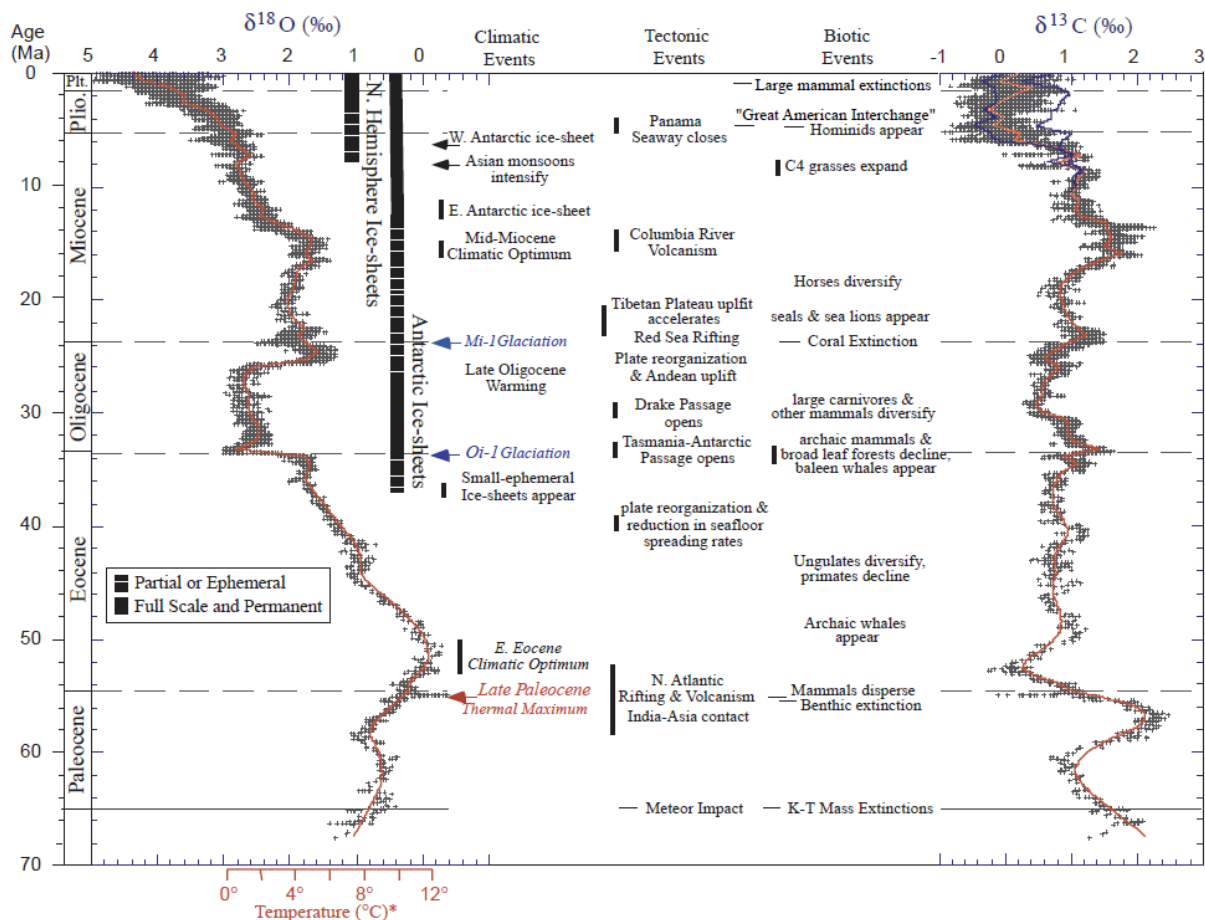


Figure 11. A long term view of benthic foraminifera stable isotope data. Along with important events that occurred during this time. From Zachos et al. 2001.

## 6 Conclusions

There are a few definite conclusions that can be drawn from the stable isotope records at Site 757 and 756 produced for this thesis project. But there are also some more speculative conclusions that would have to be confirmed or denied by further investigation. Worth noting is that it is hard to draw conclusions about large-scale oceanic and global processes from stable isotope records from one or two sites alone and this new data will hopefully be put into an even larger perspective in the future. However the conclusions that can be drawn from this investigation are that:

- At site 757B it was possible to reproduce the two step stable isotope shift that characterizes the EOT globally. The total  $\delta^{18}\text{O}$  shift recorded is a 0.8‰ increase, slightly lower than the expected >1‰ increase that has been established for the EOT in the past.
- To precisely constrain the EOT in terms of its timing it would be necessary to use a more finely tuned age model. It seems that assuming a constant sedimentation rate in the age model is not sufficient at site 757 because of the large difference in sedimentation rate after the E-O boundary, 5.5m m.y<sup>-1</sup> average in the Eocene to 2.0m m.y<sup>-1</sup> average in the Oligocene.
- The stable isotope data indicates that it may be possible to compare different species of the *Cibicidoides* genus, at the very least *Cibicidoides havanensis* and *Cibicidoides mundulus*. However more detailed studies would have to be conducted to confirm that the result at this site is not an aberration compared to other sites. In addition it appears as if internal variation in *Cibicidoides havanensis* individuals is low, this may make it possible to conduct stable isotope analysis at sites where there are few specimens available without compromising the precision of the method.
- The results does not indicate that the Oi-1 shift becomes larger when the sampling resolution is increased. Instead the difference in magnitude might be explained by the sites location in relation to what water mass affected that area at the E-O boundary. My theory is that TISW affected the northern more shallow sites (757, 756) and AAIW affected the southern deeper sites (744, 748), investigated by Zachos et al. (1992). However this conclusion is speculative at best.

It is clear that the Indian Ocean, like any other ocean basin, is a dynamic and changing system with its own trends and rhythms, as well as aberrations. If put into a larger perspective I believe that it is important to gain knowledge of past climates, to understand what the thresholds for large scale changes are, so that society get the chance to adapt to or perhaps avoid them completely.

## **Acknowledgements**

I would like to thank my supervisor Dr. Helen Coxall for her support and guidance that has helped me succeed with this project. Also her extensive knowledge and positive attitude has been a constant source of inspiration and motivation for me. I would also like to thank laboratory engineer Heike Siegmund and research engineers Klara Hajnal and Marianne Ahlbom. Siegmund for her assistance with the stable isotope analysis, Hajnal for providing and instructing me in the procedure of washing sediments and Ahlbom for instructing me in how to use the SEM. Finally I would like to thank my colleague Tomas Schedwin for his hard work producing an age model for site 757B and allowing me the use of his work so I was able to correlate my data with age.

## References

- Coxall, H. K., & Pearson, P. N., 2007, The Eocene-Oligocene transition, in Williams, M., Hayward, A., Gregory, J., and Schmidt, D. N., eds., Deep time perspectives on climate change: Marrying the signal from computer models and biological proxies: London, *Geological Society Special Publication*, p. 351-387.
- Coxall, H. K., and P. A. Wilson, 2011, Early Oligocene glaciation and productivity in the eastern equatorial Pacific: Insights into global carbon cycling, *Paleoceanography*, 26, PA2221, doi:10.1029/2010PA002021.
- Coxall, H. K., Wilson, P. A., Pälike, H., Lear, C. H., & Backman J. 2005. Rapid stepwise onset of Antarctic glaciation and deeper calcite compensation in the Pacific Ocean. *Nature* 433, 53–57.
- DeConto, R. M. & D. Pollard ,2003. Rapid Cenozoic glaciation of Antarctica induced by declining atmospheric CO<sub>2</sub>. *Nature* 421 (6920), 245–249.
- G. Nelson Eby, 2004, Principles of Environmental Geochemistry. Belmont USA: Brooks/Cole, chapter 6, pages 181-183. ISBN: 978-0-12-229061-9
- Katz, M.E., Miller, K.G., Wright, J.D., Wade, B.S., Browning, J.V., Cramer, B.S. & Rosenthal Y., 2008, Stepwise transition from the Eocene greenhouse to the Oligocene icehouse. *Nature Geoscience* 179, 1-5.
- Kennett, J., 1977. Cenozoic evolution of Antarctic glaciation, the circum-Antarctic Ocean, and their impact on global paleoceanography. *Journal of geophysical reasearch* 82 (27), 3843–3860.
- Morkhoven, F.P.C.M. van, Berggen, W.A., Edwards A.S., 1986, Cenozoic Cosmopolitan Deep-Water Benthic Foraminifera. Bull. Centres Rech. Explor. -Prod. Elf-Aquitaine, Mem. 11; Pau.
- Royer, J., Peirce, J.W. & Weissel J.K., 1989, Tectonic Constraints on the Hot-Spot Formation of Ninetyeast Ridge. In Weissel, J., Peirce, J., Taylor, E., Alt, J., et al., *Proc. ODP Sci. Results*, 121: College Station, TX (Ocean Drilling Program). 763-776.
- Shipboard Scientific Party, 1989. Site 757. In Peirce, J., Weissel, J., et al., *Proc. ODP, Init. Repts.*, 121: College Station, TX (Ocean Drilling Program), page 305-358.
- St. John, K., Leckie, R. M., Pund, K., Jones, M. & Kriisek, L. 2012, Reconstructiong Earth's Climate History – Inquiry-based Exercises for Lab and Class. West Sussex United Kingdom: John Wiley & Sons, Ltd. Chapter 6, pages 206-211. ISBN: 978-0-470-65085-5
- Wright, A. & Miller, K. G. 1993. Southern ocean influences on late Eocene to Miocene deepwater circulation. The Antarctic paleoenvironment: A perspective on global change Antarctic research series, 1–25.
- Zachos, J. C., Rea, D. K., Seto, K., Nomura, R., & Niitsuma, N., 1992, Paleogene and Early Neogene Deep Water Paleoceanography of the Indian Ocean as Determined from

Benthic Foraminifer Stable Carbon and Oxygen Isotope Records, in Duncan, R. A., Rea, D. K., Kidd, R. B., von Rad, U., & Weissel, J. K., eds., Synthesis of Results from Scientific Drilling in the Indian Ocean: Washington, D. C, *American Geophysical Union*.

Zachos, J. C., Quinn, T. M., & Salamy, K. A., 1996, High-resolution (104 years) deep-sea foraminiferal stable isotope records of the Eocene-Oligocene climate transition: *Paleoceanography*, v. 11, no. 3, p

Zachos, J. C., Pagani, M., Sloan, L. C., Thomas, E., & Billups, K., 2001, Trends, rhythms, and aberrations in global climate 65 Ma to present: *Science*, v. 292, no. 5513, p. 686-693.

# Appendix

## A. Stable Isotope Data

### Site 757B

Table 1 Stable isotope data for all samples at site 757B, including the weight that was measured prior to stable isotope analysis.

Depth (mbsf)	Sample Name + Depth Sample Source (cm)	Isotope analysis sample nr	Weight (mg)	Specimens Used (no.)	Species	$\delta^{13}\text{C}$ . ‰ VPDB	$\delta^{18}\text{O}$ . ‰ VPDB	Notes
110.55	757B 13H-1, 5-7	1	0.173	3	<i>C. havanensis</i>	0.83	1.92	
110.85	757B 13H-1, 35-37	2	0.290	3	<i>C. havanensis</i>	0.90	1.97	
111.15	757B 13H-1, 65-67	3	0.280	3	<i>C. havanensis</i>	0.85	1.75	
111.39	757B 13H-1, 89-91	4	0.318	3	<i>C. havanensis</i>	0.94	1.94	
111.86	757B 13H-1, 136-138	49	0.255	2	<i>C. havanensis</i>	0.81	2.04	
112.15	757B 13H-2, 15-17	50	0.283	3	<i>C. havanensis</i>	1.00	1.94	
112.42	757B 13H-2, 42-44	62	0.270	3	<i>C. havanensis</i>	1.13	1.83	
112.77	757B 13H-2, 77-79	21	0.213	2	<i>C. havanensis</i>	1.15	1.91	
113.03	757B 13H-2, 103-105	22	0.222	2	<i>C. havanensis</i>	1.14	1.85	
113.35	757B 13H-2, 135-137	63	0.264	3	<i>C. havanensis</i>	1.14	1.86	
113.65	757B 13H-3, 15-17	51	0.205	2	<i>C. havanensis</i>	1.12	1.77	
113.94	757B 13H-3, 44-46	26	0.228	2	<i>C. havanensis</i>	1.17	1.89	
114.29	757B 13H-3, 79-81	7	0.292	3	<i>C. havanensis</i>	1.13	1.82	
114.56	757B 13H-3, 106-108	25	0.186	2	<i>C. havanensis</i>	1.25	1.88	
114.86	757B 13H-3, 136-138	33	0.269	3	<i>C. havanensis</i>	0.92	1.88	
115.15	757B 13H-4, 15-17	8	0.265	3	<i>C. havanensis</i>	1.07	2.02	
115.46	757B 13H-4, 46-48	23	0.237	2	<i>C. havanensis</i>	1.15	1.90	
115.75	757B 13H-4, 75-77	24	0.218	2	<i>C. havanensis</i>	1.16	1.81	
116.05	757B 13H-4, 105-107	5	0.306	3	<i>C. havanensis</i>	1.28	1.81	
116.35	757B 13H-4, 135-137	34	0.242	3	<i>C. havanensis</i>	1.23	1.77	
116.65	757B 13H-5, 15-17	35	0.248	2	<i>C. havanensis</i>	1.24	2.04	
116.93	757B 13H-5, 43-45	6	0.244	3	<i>C. havanensis</i>	1.27	1.86	
117.25	757B 13H-5, 75-77	36	0.250	2	<i>C. havanensis</i>	1.26	1.57	
117.61	757B 13H-5, 111-113	37	0.214	2	<i>C. havanensis</i>	1.24	1.69	
117.87	757B 13H-5, 137-139	52	0.305	3	<i>C. havanensis</i>	1.43	2.12	
118.18	757B 13H-6, 18-20	38	0.301	3	<i>C. havanensis</i>	1.41	1.81	
118.48	757B 13H-6, 48-50	41	0.275	3	<i>C. havanensis</i>	1.65	1.91	
118.77	757B 13H-6, 77-79	53	0.267	3	<i>C. havanensis</i>	1.66	2.13	
119.08	757B 13H-6, 108-110	42	0.260	3	<i>C. havanensis</i>	1.61	1.91	
119.36	757B 13H-6, 136-138	45	0.224	3	<i>C. havanensis</i>	1.56	1.94	
119.56	757B 13H-7, 6-8	60	0.202	2	<i>C. havanensis</i>	1.36	1.54	
120.22	757B 14H-1, 12-14	58	0.227	3	<i>C. havanensis</i>	1.05	1.46	
120.54	757B 14H-1, 44-49	61	0.230	2	<i>C. havanensis</i>	1.19	1.56	
120.76	757B 14H-1, 66-68	13	0.183	3	<i>C. havanensis</i>	1.21	1.58	
121.2	757B 14H-1, 110-112	14	0.226	3	<i>C. havanensis</i>	1.18	1.60	
121.45	757B 14H-1, 135-137	59	0.260	3	<i>C. havanensis</i>	1.18	1.55	

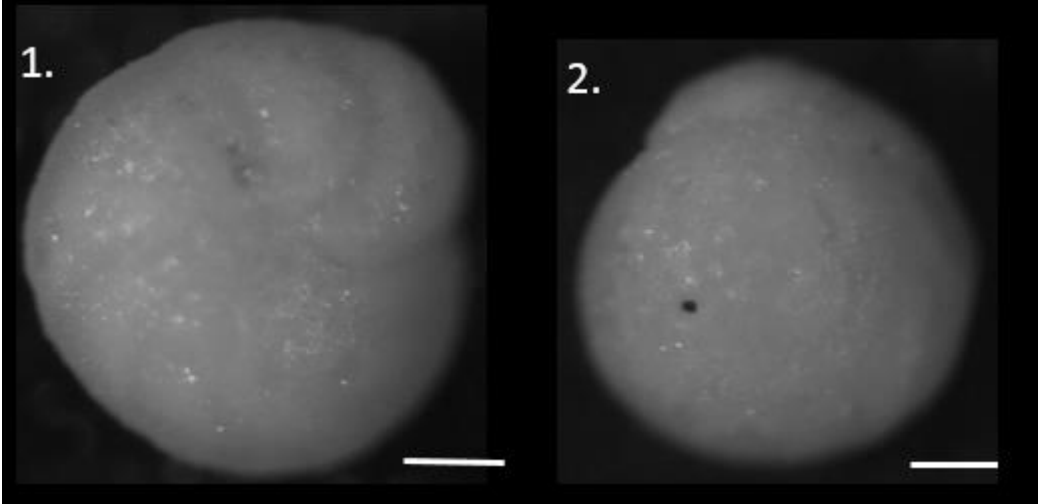
121.75	757B 14H-2, 15-17	46	0.199	3	<i>C. havanensis</i>	0.84	1.47	
122.05	757B 14H-2, 45-47	56	0.242	3	<i>C. havanensis</i>	0.76	1.28	
122.38	757B 14H-2, 78-80	43	0.220	3	<i>C. havanensis</i>	1.05	1.38	
122.65	757B 14H-2, 105-107	57	0.239	3	<i>C. havanensis</i>	1.06	1.38	
122.97	757B 14H-2, 137-139	44	0.254	3	<i>C. havanensis</i>	1.15	1.25	
123.25	757B 14H-3, 15-17	19	0.283	3	<i>C. havanensis</i>	1.00	1.47	
123.55	757B 14H-3, 45-47	15	0.259	3	<i>C. havanensis</i>	1.00	1.47	
123.78	757B 14H-3, 68-70	39	0.218	3	<i>C. havanensis</i>	1.18	1.05	
124.21	757B 14H-3, 111-113	40	0.265	3	<i>C. havanensis</i>	1.10	1.20	
124.46	757B 14H-3, 136-138	16	0.153	3	<i>C. havanensis</i>	1.06	1.37	
124.75	757B 14H-4, 15-17	20	0.293	3	<i>C. havanensis</i>	1.00	1.41	
125.05	757B 14H-4, 45-47	31	0.311	3	<i>C. havanensis</i>	1.05	1.46	
125.27	757B 14H-4, 67-69	9	0.200	3	<i>C. havanensis</i>	1.04	1.35	
125.65	757B 14H-4, 105-107	10	0.249	3	<i>C. havanensis</i>	1.05	1.33	
125.95	757B 14H-4, 135-137	32	0.193	3	<i>C. havanensis</i>	1.13	1.41	
126.25	757B 14H-5, 15-17	54	0.215	3	<i>C. havanensis</i>	1.14	1.22	
126.55	757B 14H-5, 45-47	17	0.171	3	<i>C. havanensis</i>	1.17	1.43	
126.85	757B 14H-5, 75-77	18	0.173	3	<i>C. havanensis</i>	1.22	1.31	
127.15	757B 14H-5, 105-107	47	0.217	3	<i>C. havanensis</i>	1.22	1.14	
127.45	757B 14H-5,135-137	48	0.302	3	<i>C. havanensis</i>	1.15	1.34	
127.75	757B 14H-6, 15-17	55	0.191	3	<i>C. havanensis</i>	1.22	1.17	
128.05	757B 14H-6, 45-47	27	0.236	3	<i>C. havanensis</i>	1.24	1.25	
128.35	757B 14H-6, 75-77	28	0.299	3	<i>C. havanensis</i>	1.20	1.34	
128.55	757B 14H-6, 95-97	11	0.192	3	<i>C. havanensis</i>	1.22	1.16	
128.95	757B 14H-6, 135-137	29	0.203	3	<i>C. havanensis</i>			
129.25	757B 14H-7, 15-17	30	0.191	3	<i>C. havanensis</i>	1.19	1.17	
129.54	757B 14H-CC, 6-8	12	0.190	3	<i>C. havanensis</i>	1.24	1.24	
111.15	757B 13H-1, 65-67	64	0.176	2	<i>C. mundulus</i>	1.05	1.87	Extra C.m
111.86	757B 13H-1, 136-138	65	0.296	3	<i>C. mundulus</i>	1.09	2.06	Extra C.m
112.15	757B 13H-2, 15-17	66	0.132	3	<i>C. mundulus</i>	1.12	1.76	Extra C.m
129.25	757B 14H-7, 15-17	67	0.131	3	<i>C. mundulus</i>	1.23	1.38	Extra C.m
128.95	757B 14H-6, 135-137	68	0.189	3	<i>C. mundulus</i>	1.29	1.41	Extra C.m
114.56	757B 13H-3, 106-108	69	0.249	2	<i>C. havanensis</i>	0.98	1.77	Extra C.h
114.86	757B 13H-3, 136-138	70	0.271	3	<i>C. havanensis</i>	1.10	1.88	Extra C.h
126.85	757B 14H-5, 75-77	71	0.157	3	<i>C. havanensis</i>	1.22	1.25	Extra C.h
127.15	757B 14H-5, 105-107	72	0.235	3	<i>C. havanensis</i>	1.34	1.16	Extra C.h
127.45	757B 14H-5, 135-137	73	0.179	3	<i>C. havanensis</i>	1.11	0.97	Extra C.h

## Site 756C

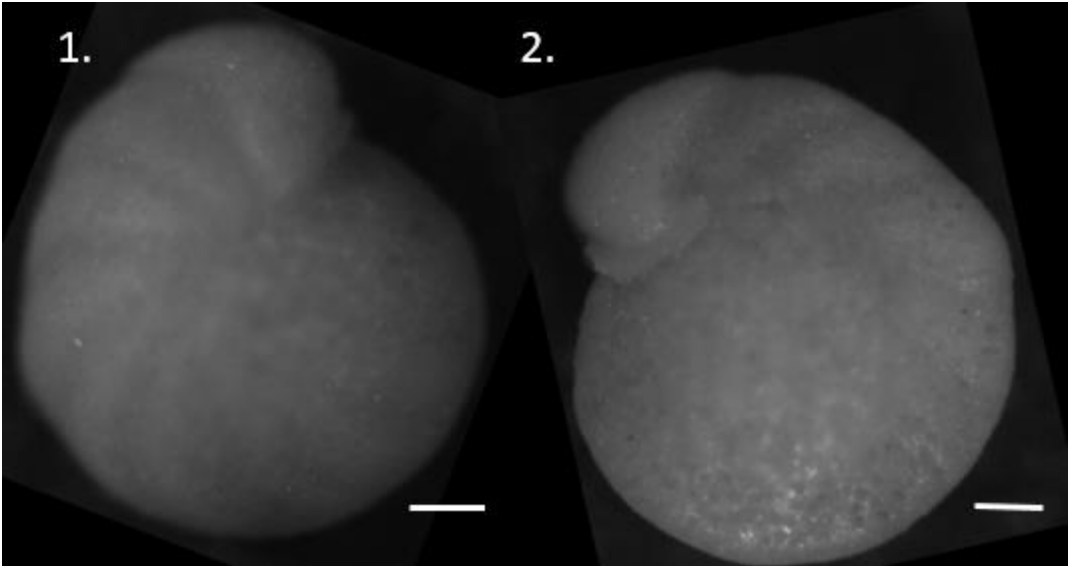
Table 2. Stable isotope data for all samples measured at site 756C, including the weight that was measured prior to stable isotope analysis.

Depth (mbsf)	Sample Name + Top (cm)	Isotope analysis sample nr	Weight (mg)	Specimens Used (no.)	Species	$\delta^{13}\text{C}$ , ‰ VPDB	$\delta^{18}\text{O}$ , ‰ VPDB	Notes
124.8	756C 6X-4, 10	74	0.232	3	<i>C.mundulus</i>	1.40	0.94	
125.3	756C 6X-4, 53	75	0.268	3	<i>C.mundulus</i>	1.29	0.96	
125.92	756C 6X-4, 122	78	0.231	3	<i>C.mundulus</i>	1.18	0.90	
126.56	756C 6X-5, 35.5	79	0.269	3	<i>C.mundulus</i>	1.00	0.70	
130.21	756C 7X-1, 41	76	0.246	3	<i>C.mundulus</i>	1.27	0.62	
130.95	756C 7X-1, 115	77	0.217	3	<i>C.mundulus</i>	1.16	0.64	
131.78	756C 7X-2, 48	80	0.276	3	<i>C.mundulus</i>	1.35	0.93	
132.45	756C 7X-2, 115	81	0.235	3	<i>C.mundulus</i>	1.29	0.73	
133.2	756C 7X-3, 40	82	0.242	3	<i>C.mundulus</i>	1.34	0.76	
133.95	756C 7X-3, 115	83	0.196	3	<i>C.mundulus</i>	1.28	0.71	
134.65	756C 7X-4, 35	87	0.270	3	<i>C.mundulus</i>	1.31	0.89	
135.4	756C 7X-4, 110	86	0.299	3	<i>C.mundulus</i>	1.37	0.69	
136.3	756C 7X-5, 50	85	0.277	3	<i>C.mundulus</i>	1.40	0.62	
136.9	756C 7X-5, 110	84	0.273	3	<i>C.mundulus</i>	1.26	0.47	
137.8	756C 7X-6, 50	90	0.252	3	<i>C.mundulus</i>	1.45	0.78	
139.5	756C 8X-1, 10	91	0.241	3	<i>C.mundulus</i>	1.29	0.80	
140.55	756C 8X-1, 115	92	0.164	3	<i>C.mundulus</i>	1.11	0.72	
141.07	756C 8X-2, 17	93	0.260	3	<i>C.mundulus</i>	1.04	0.97	
141.9	756C 8X-2, 100	88	0.294	3	<i>C.mundulus</i>	1.19	0.90	
142.65	756C 8X-3, 25	89	0.305	3	<i>C.mundulus</i>	1.13	1.01	

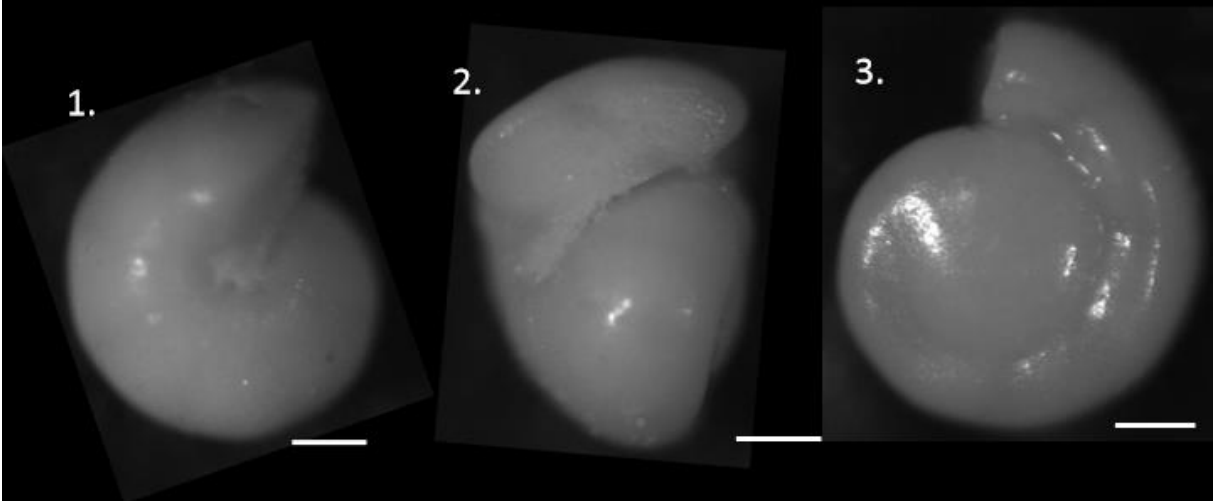
**B Microscope View of Picked Benthic Species**



Appendix B.1. Microscope view of *Cibicidoides havanensis*. (1) Umbilical side, (2) Spiral side. Scale bar 100µm.



Appendix B.2. Microscope view of *Cibicidoides mundulus*. (1) Umbilical side, (2) Spiral side. Scale bar 100µm.



Appendix B.3. Microscope view of *Gyroidinoides Sp.* (1) Umbilical side, (2) Edge view, (3) Spiral side. Scale bar 100µm.